The Effect of Backscatter Anisotropy in Assessing Hepatic Steatosis Using Ultrasound Hepatorenal Index

Jing Gao, MD, Ben Wilde, DO, Oliver D. Kripfgans, PhD, Johnson Chen, MD, Jonathan M. Rubin, MD, PhD

Received February 3, 2025, from the Montana College of Osteopathic Medicine, Rocky Vista University, Billings, MT, USA (J.G., B.W.); Department of Radiology, University of Michigan, Ann Arbor, MI, USA (O.D.K., J.M.R.); and Department of Radiology, Weill Cornell Medicine, New York, NY, USA (J.C.). Manuscript accepted for publication February 11, 2025.

The authors thank Canon Medical Systems for the consigned ultrasound equipment and research funds to support the study.

Address correspondence to Jing Gao, MD, Ultrasound Research and Education, Rocky Vista University, Montana College of Osteopathic Medicine, 4130 Rocky Vista Way, Billings, MT 59106, USA.

E-mail: jgao@rvu.edu

Abbreviations

AC, attenuation coefficient; AUROC, area under the receiver operating characteristic curve; CKD, chronic kidney disease; CT, computed tomography; HRI, hepatorenal index; ICC, intraclass correlation coefficient; IQR, interquartile range; MASLD, metabolic dysfunction-associated fatty liver disease.; MRI-PDFF, magnetic resonance imaging-based proton density fat fraction.; ROI, region of interest; SOS, speed of sound; QUS, quantitative ultrasound

doi:10.1002/jum.16669

Objectives—To discuss challenges in assessing hepatic steatosis using ultrasound hepatorenal index (HRI).

Methods—We retrospectively analyzed HRI and liver magnetic resonance imaging-based proton density fat fraction (MRI-PDFF) in 134 adult participants (53 men and 81 women, mean age 55 years). The diagnostic performance of HRI for determining hepatic steatosis was tested by the area under the receiver operating characteristic curve (AUROC) using liver MRI-PDFF as the reference. Regression plots were employed to compare the sampling sites in liver and kidney that were used to calculate HRIs.

Results—In 11 of 134 cases (8.2%), we failed to acquire HRI measurements. In the remaining 123 cases, AUROC for HRI (cutoff: 1.69 ± 0.13 [mean $\pm$ standard deviation]) for defining the HRI threshold for diagnosing hepatic steatosis was 0.83. In 60 of 123 cases (49%) with HRI measurement IQR/median >0.3, slopes of the regression lines in the liver showed backscatter intensity changes consistent with signal attenuation. However, in the kidney, the backscatter intensity was inverted yielding position-dependent HRI cutoff values, mid-pole $= 2.24 \pm 0.20$ and upper pole $= 1.08 \pm 0.16$.

Conclusions—HRI is used to estimate liver steatosis based on backscattered ultrasound. In order to compensate for effects such as body habitus and transducer frequency, the liver backscatter is divided by backscatter from a corresponding region at the same depth in the right renal cortex. Theoretically, this compensation should make HRI sampling position independent. Yet, due to renal cortical backscatter anisotropy, this compensation method does not work in general, potentially producing inaccurate liver fat estimates.

Key Words—anisotropy; backscatter intensity; hepatorenal index; metabolic dysfunction associated fatty liver disease; ultrasound

Metabolic dysfunction-associated steatotic liver disease (MASLD) is a common chronic liver disorder affecting approximately 30% of the world's population. It is a leading cause of cirrhosis, liver failure, and hepatocellular carcinoma if left untreated.[1] Furthermore, MASLD is closely linked to the development of cardiovascular disease and chronic kidney disease (CKD).[2,3] Therefore, detecting the early, reversible stages of hepatic steatosis is crucial for preventing disease progression and achieving the best outcomes for patients with MASLD.[4]

Computed tomography (CT) attenuation and magnetic resonance imaging-based proton density fat fraction (MRI-PDFF)

© 2025 American Institute of Ultrasound in Medicine.

have been used to assess hepatic steatosis. These techniques are preferred over serum chemical markers and liver biopsy, which are either insensitive or invasive.[5] However, CT is not suitable for assessing liver steatosis due to unjustifiable radiation exposure. Diagnosis with CT occurs when the exam is performed for other purposes. MRI-PDFF is recommended as the reference standard for screening and monitoring MASLD.[6–8] Recently, quantitative ultrasound biomarkers (QUS), including attenuation coefficient (AC), backscatter coefficient (BSC), and speed of sound (SOS), have become commercially available for assessing hepatic steatosis.[9]

In lieu of the more sophisticated methods for assessing liver fat, hepatorenal index (HRI) has been used to assess hepatic steatosis for decades on conventional B-mode ultrasound scans.[9–12] HRI represents a comparison of the echogenicity (backscatter intensity) in regions of interest (ROI) in the liver parenchyma and a corresponding area at the same distance from the transducer in the renal cortex (HRI = mean backscatter intensity in liver ROI/mean backscatter intensity in renal cortex ROI). The matching ROIs in the liver and kidney are chosen to compensate for scanning parameters such as transducer frequency and attenuation due to overlying tissues. Included in the HRI image parameter compensation is the assumption that liver and kidney backscatter is directionally independent, that is, isotropic. Normally, the backscatter intensity in the liver parenchyma appears similar to that in the renal cortex. Excessive fat accumulation in hepatocytes increases acoustic backscatter, resulting in higher liver backscatter intensity, and consequently, a higher HRI in patients with hepatic steatosis.[8]

The diagnostic performance of HRI for determining hepatic steatosis remains controversial.[10] The area under the receiver operating characteristic curve (AUROC) of HRI for determining ≥mild hepatic steatosis widely ranges from 0.71 to 0.90.[11,12] A moderate correlation has been found between HRI and liver biopsy and between HRI and MRI-PDFF (r = 0.70–0.83).[11,13,14] However, intra-observer repeatability and inter-observer reproducibility in performing HRI measurements are poor to moderate.[15] The intraclass correlation coefficient (ICC) for measuring HRI in participants with normal livers was 0.78 (95% confidence interval 0.47–0.91) and in participants with steatotic livers was 0.85 (95% confidence interval 0.61–0.94).[15] Despite these limitations, B-mode ultrasound-based HRI remains a frequently used method for screening hepatic steatosis due to its high availability, from hand-held devices to state-of-the-art scanners, as newly developed QUS biomarkers are still under clinical investigation.

The aim of the study was to analyze the diagnostic performance of HRI in determining hepatic steatosis and discuss common technical challenges in measuring HRI through a retrospective review.

Material and Methods

Data Review

The study is a retrospective review. We obtained approval from the Institutional Review Board (IRB) and informed consent from participants in the initial pilot study (IRB: 2019-0009). Between 2019 and 2022, the initial study for screening adult MASLD was conducted using multiparametric QUS and liver MRI-PDFF. QUS biomarkers were measured using a curvilinear transducer (PVI-475BX, 1.8–6.2 MHz, Aplio i800, Canon Medical Systems USA, Tustin, CA, USA) on participants with known or suspected MASLD. We reviewed mean, standard deviation (SD), median, interquartile range (IQR), and IQR/median of HRI in the report pages from the same participants. Fasting liver MRI-PDFF (3.0 T, Discovery MR 750, General Electric Healthcare, Milwaukee, WI, USA) was performed within 30 days before or after the ultrasound scan. The average of 9 PDFF values in each liver interpreted by board-certified abdominal radiologists was used for analysis.

Ultrasound HRI

Initially, HRI was measured 4 times using machine presets designed by the ultrasound manufacturer. The operator measured HRI by placing 2 ROI, 1 in the liver and the other in the right renal cortex at the same depth. Four HRI values were measured in different liver-renal sites. The mean, SD, median, IQR, and IQR/median from the 4 HRI were calculated using online software and displayed on the report page. Using the review function on the scanner (Canon Medical Systems), we first searched for the causes of HRI measurement failure. We then calculated the number of cases with an IQR/median of HRI value >0.3 on report pages, paying special

attention to measurement ROI depth and ROI location that may have contributed to HRI IQR/median >0.3 in the initial study. The previous HRI value was automatically deleted once "Intensity Ratio" function for measuring HRI was activated, which allowed the operator to place new circle-shaped ROIs (10 mm in diameter) in the liver parenchyma and right renal cortex to measure HRI (Figure 1). The backscatter intensity ratio of the liver to right renal cortex was based on grayscale intensity counted in both ROIs using histograms.[16] Manufacturer-machine settings, such as time gain compensation (TGC), dynamic range, harmonic imaging, and speckle reduction can be compensated for prior to measuring HRI. Theoretically, HRI measurements should be consistent despite different user machine setting preferences during data collection.

To assess the possibility that normalization of the HRI was sampling position dependent, we used histograms to estimate mean pixel backscatter intensities in the mid-pole and upper pole of the right renal cortex, and again in the corresponding positions in the liver in the 60 subjects with HRIs whose IQR/median measurements were >0.3 (Figure 2). By hypothesis, the HRI measurements should be sampling position independent, and hence there should be no difference in HRI values based on normalization using either the upper or mid-pole measurements.

Statistical Analysis

We used several methods to evaluate the effects of sampling sites within the liver and right kidney to assess sources of variability in HRI measurements. For each subject for which the IQR/median for the HRI >0.3, we plotted the mean backscatter intensity estimate in the mid-pole versus the upper pole of the right kidney, and we performed a similar plot for the corresponding regions in the liver. We separated these groups into the normal population and those with MRI-PDFF measurements showing liver fat levels >5%. We then calculated a linear regression for each plot and calculated the slope of the regression using a Matlab routine (The MathWorks, Natick, MA, USA). We chose to force the regression line through the origin, which is consistent with the physical reality that as scanning gain/output is decreased to zero, all of the backscatter values must go to zero as well. We used the 95% confidence limits of the slopes of the regression to see how well the data would fit the normalization hypotheses required for HRI measurements. That is, if the 95% confidence intervals of the slopes of the linear regressions for the corresponding positions in the liver and right renal cortex overlapped, then we would conclude that the HRI compensation was valid.

Next, we assessed the diagnostic performance of HRI for determining ≥mild hepatic steatosis (MRI-PDFF >5%) using areas under the AUROC. AUROC

Figure 1. A–**D**, The hepatorenal index (HRI) is measured on a subject with severe hepatic steatosis (liver MRI-PDFF 21%). The value of HRI is strongly affected by the relation between the direction of the sound beam and the renal cortical tissue. The HRI value is 6.27 in the mid pole where the direction of the sound beam tends to be parallel to the medullary rays in the renal cortex (**A**). Following more angulation between the sound beam and the cortical tissue, HRI tends lower (HRI = 3.27, **B**; HRI = 2.54, **C**). The lowest HRI value measures 1.70 in the upper pole of the kidney where the sound beam is nearly perpendicular to the medullary rays (**D**).

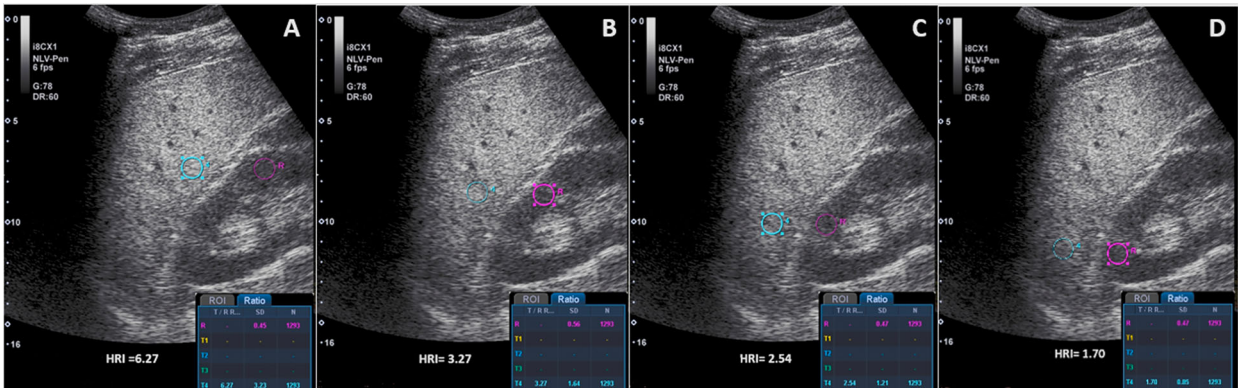

was estimated using a Matlab routine with an MRI-PDFF fat percentage estimate of 5% as the cutoff gold standard. We then determined the standard deviations of the AUROC estimates using a boot-strapping technique where 30% of the original HRI data for each sampling site was randomly selected for ROC calculation. Data used for each boot-strapped ROC calculation could be reused in subsequent calculations; however, each ROC calculation was generated from a unique subset of HRI measurements. For each analyzed site, 100 boot-strap curves were generated in order to calculate the corresponding standard deviation.

We estimated the cutoff thresholds for ROC curves using the same boot-strapped data to calculate cutoff means and standard deviations. We employed the Index of Union (the optimal value is close to the area under ROC and minimal difference between sensitivity and specificity) method for determining the cutoff.[17,18] Means and standard deviations for the cutoffs were compared using 2-tailed *t*-test (Matlab). A P value <.05 is considered statistically significant for all comparisons.

Results

Demographic information of the participants is listed in Table 1. In the reviewed 134 cases, the failure rate for acquiring HRI measurements was 8.2% (11/134). The IQR/median for HRI measurement was 0.32 ± 0.16, with 49% (60/123) of cases having an IQR/median >0.3. Among these 60 cases with IQR/median >0.3, 95% of the highest HRI values were measured at the depth corresponding to the kidney mid-pole, and 92% of the lowest HRI values were measured at the depth corresponding to the kidney upper pole, even if both measurement ROIs in the liver and right renal cortex for individual participant were placed at the same depth from the skin (Figure 1).

Plots with regression lines for the 4 groups of subjects with HRI estimates having IQR/mean >0.3 are shown in Figure 3. Neither of the 95% confidence intervals for the slopes of the regression lines for the matching pairs for the 2 cases, normal livers and steatotic livers, overlapped (Figure 3). That is the slopes of regression for the normal liver and the corresponding right renal cortex and the steatotic

Table 1. Demographic Information and Ultrasound Performance in 134 Participants

		Note
Number of cases	134	11 excluded from analysis
Age (year)	55 ± 17	
Male/Female	53/81	
BMI (kg/cm^2)	31.67 ± 6.26	
Measurement failure and causes	11/134 (8.2%)	
Ascites	n = 4	Renal cortex separating from the liver
Kidney low location	n = 3	Cortex and liver not at same depths
Chronic kidney disease >Stage 3	n = 3	Backscatter in renal cortex >liver
Multiple cysts in right kidney	n = 1	No normal renal cortex adjacent to liver

BMI, body mass index; measurement failure, backscatter intensity of liver and renal cortex cannot be measured at the same image depth.

Figure 2. A–D, Mean liver pixels (backscatter intensity) of 93.69 (A) and 94.25 (B) (**A**) and mean renal cortex pixels of 66.92 (A) and 88.82 (B) (**B**) are measured in a participant with the normal liver (liver MRI-PDFF 4.2%). Mean liver pixels of 108.29 (A) and 110.094 (B) (**C**) and mean renal cortex pixels of 51.09 (A) and 78.44 (B) (**D**) are also measured in a participant with moderate hepatic steatosis (liver MRI-PDFF 18%). The renal cortical backscatter intensity in upper pole is higher than that in mid-pole in normal participant (88.82 versus 66.92) and the participant with hepatic steatosis (78.44 versus 51.09).

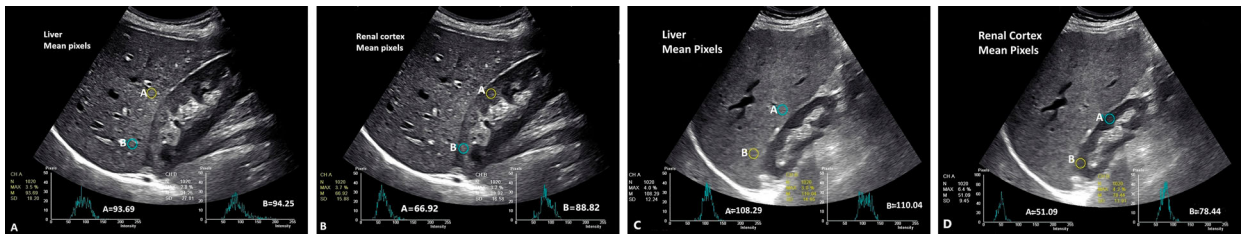

liver and the corresponding right renal cortex do not overlap. Interestingly, the slopes of the regressions in the paired positions in the liver are less than 1, but those in the kidney are greater than 1 (Figure 3).

In 123 participants, the primary operator (JG) randomly selected 4 positions in the renal cortex, between the upper pole and mid-pole, and a corresponding point for each sample in the liver to

Figure 3. Regression plots comparing mean backscattered values from selected sites in the liver and right kidney used for HRI measurements. The intensity measurements are in arbitrary units derived from the Canon scanner. Left upper plot: Compares the 2 sites in the normal liver group from which HRIs were calculated. N. Liver UP = normal liver region matched to the right kidney upper pole, N. Liver MP = normal liver region matched to the right kidney mid-pole. Right upper plot: Compares 2 sites in the right kidneys used to the normal liver positions. N. Kidney UP = upper pole samples from kidneys matched to normal liver, N. Kidney MP = mid-pole samples from right kidneys matched to normal liver. Left lower plot: Compares 2 sites in the steatotic livers from which HRIs were calculated. S Liver UP = steatotic liver samples matched to the upper pole of the right kidney, S Liver MP = steatotic liver samples matched to the MP of the right kidney. Right lower plot: Compares the sites in the right kidney used to normalize the steatotic liver positions. S. Kidney UP = upper pole samples from kidneys matched to steatotic liver. S. Kidney MP = mid-pole samples from right kidneys matched to steatotic liver. Solid black line in each plot called "bisector" has the slope of 1 and represents the positions from which the backscatter from the 2 axes would be identical. The red dashed line corresponds to the best fit line through the backscattered data where the slope is forced through the origin. Slope = slope of the dotted line with the 95% confidence intervals of the slope within parentheses.

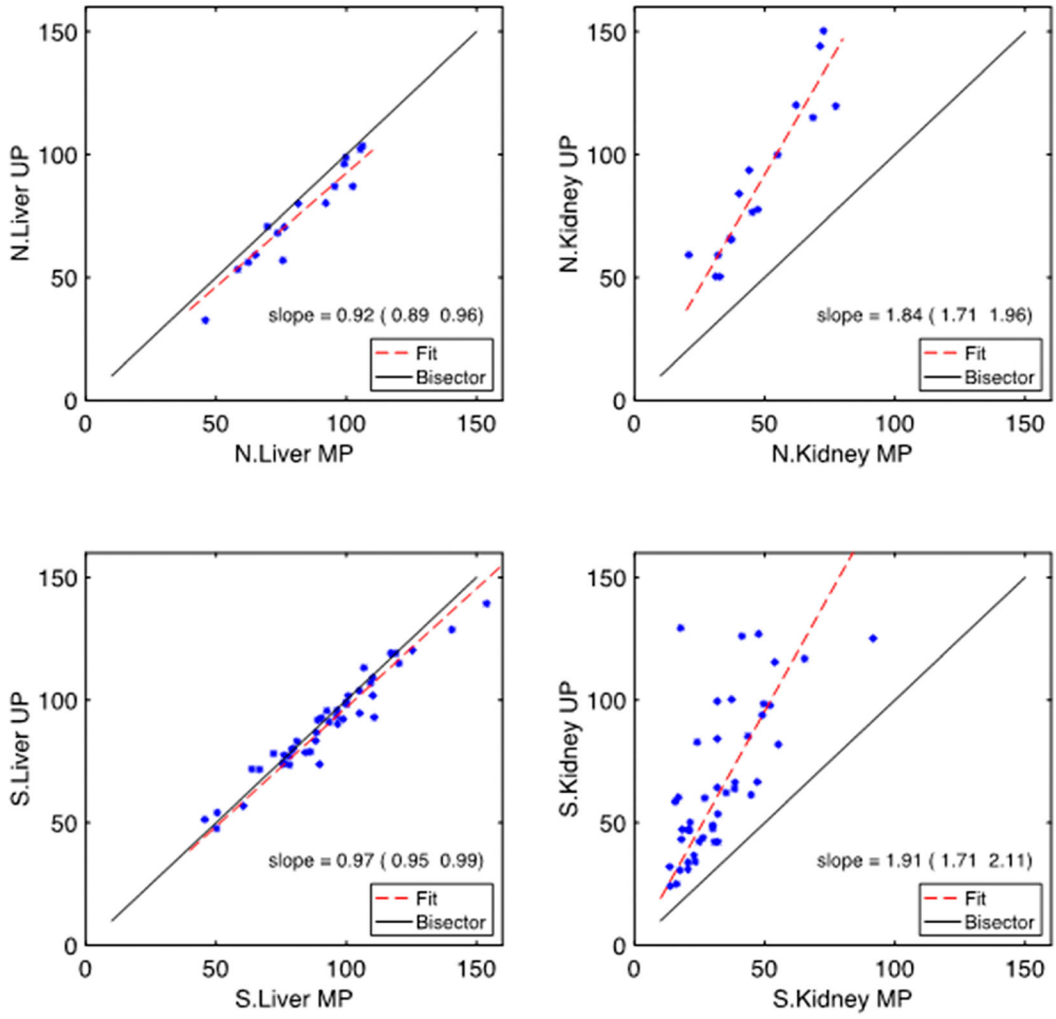

estimate the HRI. The median HRI value was used to represent these measurements. This produced an AUROC of HRI for those cases with a fatty liver (MRI-PDFF >5%) equal to 0.83 ± 0.06 (mean ± standard deviation) with an HRI of 1.69 ± 0.13 as the best cut-off value. In 60 cases with HRI IQR/Median >0.30, AUROC of HRI measured in liver-renal mid-pole and upper pole was 0.87 ± 0.08 and 0.80 ± 0.11 with the cutoff values of 2.24 ± 0.20 and 1.08 ± 0.16, respectively (Table 2, Figure 4). All of the cutoff values are highly statistically significantly different from each other ($P < .001$), and the AUROCs were statistically significantly different from each other as well ($P < .005$).

Discussion

The major finding in this study is that the normalization assumption made when employing HRI to estimate liver fat is not valid. This is strongly demonstrated by the slopes of the regression plots in Figure 3. The slopes for the ROI selected in the liver show what would be expected if sound attenuation were producing the backscatter difference between the more superficial region corresponding to the mid-pole kidney measurement and the deeper position corresponding to the upper pole measurement. In both cases with and without fatty livers, the slopes were less than 1. This is what one would expect if sound attenuation effects were modulating the liver backscatter. That is to say that the more superficial region generated more backscatter than the deeper region. The TGC curves apply a depth-dependent amplification to the backscattered ultrasound signals to compensate for sound attenuation. However, this compensation is not perfect since the regression slope is not equal to 1. By assumption, this attenuation effect would be present in the renal

Table 2. Area Under ROC of Hepatorenal Index for Determining ≥Mild Hepatic Steatosis

	Cases	Cutoff (SD)	AUROC (SD)	Sensitivity	Specificity
Random HRI	123	1.69 (0.13)	0.83 (0.06)	0.75	0.83
Mid-pole HRI	60	2.24 (0.20)	0.87 (0.08)	0.77	0.88
Upper-pole HRI	60	1.08 (0.16)	0.80 (0.11)	0.73	0.81

Mild hepatic steatosis is determined using magnetic resonance imaging-based protein density fat fraction (MRI-PDFF) >5%; AUROC, area under receiver operating characteristic curve; cut-off thresholds for ROC curves, sensitivity, and specificity were estimated using Index of Union method.[15]
HRI, hepatorenal index; SD, standard deviation.

Figure 4. A–C, The areas under the receiver operating characteristic curve of hepatorenal index, for diagnosing fatty liver are 0.83 (**A**), 0.87 (**B**), and 0.80 (**C**), for random, mid-pole, and upper pole measurement, respectively, with the corresponding cutoff values of 1.69 for random, 2.24 for mid-pole, and 1.08 for upper pole.

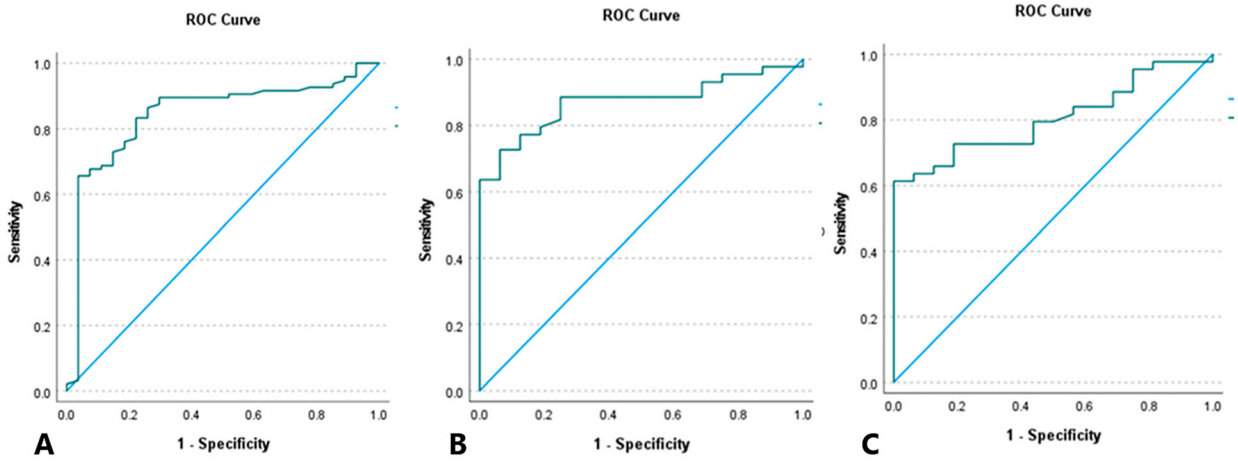

cortical measurements as well, and HRI would compensate for this.

However, the renal measurements were reversed. Not only are the slopes of regression in the kidneys significantly higher than the liver, but the slopes of the regression lines relating the 2 measurements in the right renal cortex are both greater than 1. That is the backscatter from the deeper upper pole region was higher than the more superficial mid-pole region. This cannot be due to attenuation and is most likely due to backscatter anisotropy caused by radially oriented striations in the renal cortex generated by the medullary rays and interlobar arteries.[16,19,20] In the upper pole, the medullary rays and interlobar arteries are perpendicular to the ultrasound beam when a transducer is positioned for an HRI measurement, while they are parallel to the beam when scanning the mid-pole for an HRI measurement. Therefore, the backscatter from the upper pole of the kidney is stronger than from the mid-pole even though the upper pole is deeper in the body relative to the transducer than the mid-pole.[20] This anisotropy defeats the purpose of HRI, and it strongly affects the HRI measurements making them dependent on which portion of the kidney is being used for normalization.

The effect of anisotropy on HRI measurements easily explains some of the variability in the measurement. This is demonstrated by how the HRI threshold separating the normal liver from the fatty liver populations is highly dependent on the portion of the kidney that is used to normalize the HRI measurements. For HRI to work, this threshold should be independent of the portion of the kidney used to normalize the liver measurement. Yet, the HRI thresholds for the 3 different positions in the renal cortex are significantly different from each other. Thus, using a threshold from one portion of the kidney when sampling another will lead to errors. For instance, if one used the mid-pole threshold of 2.24 when scanning the upper pole, one would have a sensitivity of about 20% and a specificity of 100% (SPSS, version 28, IBM). Thus, almost every case would be normal because there would be a large number of false negatives caused by the increased backscatter from the upper pole.

Further, the AUROCs for HRIs produced from all 3 areas in the kidney are also statistically significantly different with the mid-pole HRI having the largest AUROC, 0.87 ± 0.08. Therefore, the mid-pole of the kidney is the best region to use to normalize the liver measurement. However, this also requires that the region of the liver that can be used in the HRI measurement must match the mid-pole of the kidney in depth, and the correct HRI cutoff value $= 2.24$ must be used in the assessment. This greatly limits the portions of the liver that can use HRI to assess fat content. Normalizing an HRI measurement to the wrong part of the liver or using a cutoff value from another part of the kidney will degrade the measurement. This restriction is expressly counter to the underlying HRI hypothesis where the normalization is supposed to make HRI measurements independent of sampling position in the right renal cortex.

Limitations in the study include:

1. Operator variability: 1 senior operator scanned all participants in the initial study. Poor inter- and intra-observer reliability in measuring HRI has been observed in training studies.[15]
2. Lack of ROI placement guidelines: We measured 4 HRIs per participant following the manufacturer's recommendations. It is unclear if increasing the number of measurements would improve HRI's diagnostic performance. In addition, it is challenging to standardize the depth for measuring HRI. The anatomic relation between the liver and right kidney's upper and mid-poles significantly varies among individuals.[21] Further, this also creates issues if one wants to compensate for anisotropy by only performing HRIs at the upper or mid-poles of kidneys to account for cutoff value differences. Such a constraint would make the measurement more difficult and further limit the number of cases where HRI could be successfully applied.
3. Single-vendor scanner: The study was conducted using a scanner from a single ultrasound vendor, and comparisons with other vendors were not performed.
4. MRI-PDFF reference: MRI-PDFF was used as the reference for assessing hepatic steatosis.[22] The study did not analyze HRI's effectiveness in determining or grading liver inflammation or fibrosis due to the lack of liver histology data.

5. Limited measurement locations: HRI measurements were only taken in the right lobe of the liver near the right kidney, limiting the assessment of backscatter intensity in other liver segments.
6. Single institution: The study was a retrospective review based on data collected at a single institution.

Conclusion

We aim to discuss challenges and technical considerations to improve HRI's diagnostic performance in MASLD screening. Study results suggest that a cutoff value of HRI for assessing hepatic steatosis varies depending on where the HRI is measured. The cutoff is high in the mid-pole and low in the upper pole due to renal cortex anisotropy. Therefore, when making an HRI measurement, the liver and right renal cortex measurements not only need to be equal distance from the transducer face, but they also require specific position-dependent cutoffs for determining liver fat fractions. These position-dependent cutoffs go against the primary reason for normalizing measurements like HRI in the first place and can lead to inaccurate liver fat estimates. Hence, whenever possible, medical assessments of liver steatosis should be based on newly developed biomarkers, such as attenuation coefficients.

Data Availability Statement

The data that support the findings of this study are available on request from the corresponding author. The data are not publicly available due to privacy or ethical restrictions.

References

1. Chan WK, Chuah KH, Rajaram RB, Lim L-L, Ratnasingam J, Vethakkan SR. Metabolic dysfunction-associated steatotic liver disease (MASLD): a state-of-the-art review. *J Obes Metab Syndr* 2023; 32:197–213. https://doi.org/10.7570/jomes23052.
2. Mellemkjær A, Kjær MB, Haldrup D, Grønbæk H, Thomsen KL. Management of cardiovascular risk in patients with metabolic dysfunction-associated steatotic liver disease. *Eur J Intern Med* 2024; 122:28–34. https://doi.org/10.1016/j.ejim.2023.11.012.
3. Umbro I, Baratta F, Angelico F, Del Ben M. Nonalcoholic fatty liver disease and the kidney: a review. *Biomedicine* 2021; 9:1370. https://doi.org/10.3390/biomedicines9101370.
4. Chauhan A, Sultan LR, Furth EE, Jones LP, Khungar V, Sehgal CM. Diagnostic accuracy of hepatorenal index in the detection and grading of hepatic steatosis. *J Clin Ultrasound* 2016; 44:580–586. https://doi.org/10.1002/jcu.22382.
5. Nalbantoglu IL, Brunt EM. Role of liver biopsy in nonalcoholic fatty liver disease. *World J Gastroenterol* 2014; 20:9026–9037. https://doi.org/10.3748/wjg.v20.i27.9026.
6. Ferraioli G, Barr RG, Berzigotti A, et al. WFUMB guidelines/guidance on liver multiparametric ultrasound. Part 2: guidance on liver fat quantification. *Ultrasound Med Biol* 2024; 50:1088–1098. https://doi.org/10.1016/j.ultrasmedbio.2024.03.014.
7. Ferraioli G, Kumar V, Ozturk A, Nam K, de Korte CL, Barr RG. US attenuation for liver fat quantification: an AIUM-RSNA QIBA pulse-echo quantitative ultrasound initiative. *Radiology* 2022; 302:495–506. https://doi.org/10.1148/radiol.210736.
8. Trujillo M, Chen J, Rubin JM, Gao J. Non-invasive imaging biomarkers to assess nonalcoholic fatty liver disease: a review. *Clin Imaging* 2021; 78:22–34. https://doi.org/10.1016/j.clinimag.2021.02.039.
9. Fetzer DT, Rosado-Mendez IM, Wang M, et al. Pulse-echo quantitative US biomarkers for liver steatosis: toward technical standardization. *Radiology* 2022; 305:265–276. https://doi.org/10.1148/radiol.212808.
10. Barr RG. Ultrasound of diffuse liver disease including elastography. *Radiol Clin North Am* 2019; 57:549–562.
11. Marshall RH, Eissa M, Bluth E, Gulotta PM, Davis NK. Hepatorenal index as an accurate, simple, and effective tool in screening for steatosis. *AJR Am J Roentgenol* 2012; 199:997–1002. https://doi.org/10.2214/ajr.11.6677.
12. Webb M, Yeshua H, Zelber-Sagi S, et al. Diagnostic value of a computerized hepatorenal index for sonographic quantification of liver steatosis. *AJR Am J Roentgenol* 2009; 192:909–914.
13. Kjaergaard M, Lindvig KP, Hansen CD, Detlefsen S, Krag A, Thiele M. Hepatorenal index by B-mode ratio versus imaging and fatty liver index to diagnose steatosis in alcoholic related and non-alcoholic fatty liver diseases. *J Ultrasound Med* 2023; 42:487–496. https://doi.org/10.1002/jum.15991.
14. Tran BV, Ujita K, Taketomi-Takahashi A, Hirasawa H, Suto T, Tsushima Y. Reliability of ultrasound hepatorenal index and magnetic resonance imaging proton density fat fraction techniques in the diagnosis of hepatic steatosis, with magnetic resonance spectroscopy as the reference standard. *PLoS One* 2021; 16:e0255768. https://doi.org/10.1371/journal.pone.0255768.
15. Gao J, Lee R, Trujillo M. Reliability of performing multiparametric ultrasound in adult livers. *J Ultrasound Med* 2022; 41:699–721. https://doi.org/10.1002/jum.15751.

16. Johnson SI, Fort D, Shortt KJ, et al. Ultrasound stratification of hepatic steatosis using hepatorenal index. *Diagnostics* 2021; 11: 1443. https://doi.org/10.3390/diagnostics11081443.
17. Nahm FS. Receiver operating characteristic curve: overview and practical use for clinicians. *Korean J Anesthesiol* 2022; 75:25–36. https://doi.org/10.4097/kja.21209.
18. Unal I. Defining an optimal cut-point value in ROC analysis: an alternative approach. *Comput Math Methods Med* 2017; 2017:1–14. https://doi.org/10.1155/2017/3762651.
19. Tanpowpong N, Panichyawat S. Comparison of sonographic hepatorenal ratio and the degree of hepatic steatosis in magnetic resonance imaging-proton density fat fraction. *J Ultrasound* 2020; 20:e169–e175. https://doi.org/10.15557/JoU.2020.0028.
20. Rubin JM, Carson PL, Meyer CR. Anisotropic ultrasonic backscatter from the renal cortex. *Ultrasound Med Biol* 1988; 14:507–511.
21. Eid S, Iwanaga J, Loukas M, Oskouian R, Tubbs RS. Pelvic kidney: a review of the literature. *Cureus* 2018; 10:e2775. https://doi.org/10.7759/cureus.2775.
22. Middleton MS, Heba ER, Hooker CA, et al. Agreement between magnetic resonance imaging proton density fat fraction measurements and pathologist-assigned steatosis grades of liver biopsies from adults with nonalcoholic steatohepatitis. *Gastroenterology* 2017; 153:735–761.